An ab Initio Calculation of the Valence Excitation Spectrum of $H_2O\cdots Cl_2$: Comparison to Condensed Phase Spectra†

Ricardo Franklin-Mergarejo

Instituto Superior de Tecnologías y Ciencias Aplicadas, Ave. Salvador Allende y Luaces, Quinta de los Molinos, Plaza, Habana 10600, Aptdo. Postal 6163, Ciudad Habana, Cuba, Université de Toulouse, UPS, Laboratoire Collisions Agrégats Réactivité, IRSAMC, F-31062 Toulouse, France, and CNRS, UMR 5589, F-31062 Toulouse, France

Jesus Rubayo-Soneira

Instituto Superior de Tecnologías y Ciencias Aplicadas, Ave. Salvador Allende y Luaces, Quinta de los Molinos, Plaza, Habana 10600, Aptdo. Postal 6163, Ciudad Habana, Cuba

Nadine Halberstadt*

Université de Toulouse, UPS, Laboratoire Collisions Agrégats Réactivité, IRSAMC, F-31062 Toulouse, France, and CNRS, UMR 5589, F-31062 Toulouse, France

Tahra Ayed‡

Centro de Investigaciones Químicas, UAEM, Cuernavaca, Mor. 62210, México

Margarita I. Bernal Uruchurtu

Centro de Investigaciones Químicas, UAEM, Cuernavaca, Mor. 62210, México

Ramón Hernández-Lamoneda

Centro de Investigaciones Químicas, UAEM, Cuernavaca, Mor. 62210, México

Kenneth C. Janda

Department of Chemistry, University of California, Irvine, Irvine, California 92697-2025

Received: February 14, 2009; Revised Manuscript Received: April 8, 2009

Valence electronic excitation spectra are calculated for the $H_2O\cdots Cl_2$ dimer using state-of-the art ab initio potentials for both the ground and the valence excited states, a basis set calculation of the ground state nuclear wave funtion, and a wave packet analysis to simulate the dynamics on the excited state surface. The peak of the $H_2O\cdots Cl_2$ dimer spectrum is blue-shifted by 1250 cm^{-1} from that of the free Cl_2 molecule. This is less than the value previously estimated from vertical excitation energies but still significantly more than the blue shift in aqueous solution and clathrate−hydrate solid. Seventy percent of the blue shift is attributed to ground state stabilization, the rest to excited state repulsion. Spin−orbit effects are found to be small for this dimer. Homogeneous broadening is found to be slightly smaller for the dimer than for the free Cl_2. The reflection principle and spectrator model approximations were tested and found to be quite satisfactory. This is promising for an eventual simulation of the condensed phase spectra.

I. Introduction

The spectra of halogen molecules have long been known to be very sensitive to the local environment.[1,2] For instance, in aqueous solution, the valence excitation spectrum of Cl_2 is shifted 550 cm^{-1} to the blue from the gas phase spectrum.[3] For Br_2 and I_2 the shifts are even more dramatic, 1750 and 2820 cm^{-1}, respectively.[4,5] Although these spectral shifts have received considerable attention, no satisfactory explanation has been found. Part of the reason for this difficulty is that nearest neighbor and bulk dielectric effects are probably both important and vary in importance depending on which halogen is being studied.[6,7]

Recently, the sensitivity of the spectrum to the local environment was studied for halogen in clathrate hydrate gas−solid solutions. Clathrate hydrates consist of a solid lattice in which the water molecules form different sized cages. For instance, a 28 water molecule cage that has 12 pentagonal faces and 4 hexagonal faces with an oxygen atom at each vertex and a hydrogen atom along each edge is referred to as a $5^{12}6^4$ clathrate hydrate cage. The spectrum of Cl_2 in a 24 water molecule $5^{12}6^2$ cage is unshifted from that in the gas phase. The spectrum of

† Part of the "Robert Benny Gerber Festschrift".

* Corresponding author, Nadine.Halberstadt@irsamc.ups-tlse.fr.

‡ Permanent address: Unité de Recherche de Chimie Théorique et Réactivité, Institut Préparatoire aux Etudes d'Ingénieur d'El Manar, Campus universitaire B.P.244, El Manar II, 2092 Tunis, Tunisia.

10.1021/jp901488x CCC: $40.75
Published on Web 05/06/2009

Br_2 in the same cages is shifted by 880 cm^{-1}, only half of the shift in aqueous solution. In the larger, 28 water molecule $5^{12}6^4$ cage, the shift of the Br_2 spectrum is even smaller, 360 cm^{-1}. The shift of the I_2 spectrum in the 28 water molecule cage is 1440 cm^{-1}, about half of the shift between the gas phase and aqueous solution.

The large difference between the spectra of the halogens in aqueous solution and in the hydrate clathrates, as well as the very different shifts for the three halogens in each environment, is an interesting problem worthy of detailed investigation. We have started a program of study in which the spectra in dimers, clusters, and eventually aqueous solution will be investigated. A recent paper[8] reported a study of the two-dimensional potential energy surfaces for the ground states and singlet and triplet valence excited states of $H_2O\cdots Cl_2$ and $H_2O\cdots Br_2$. The details of the dimer potentials were found to be quite sensitive to the basis set and degree of electron correlation. Another interesting result of this study is that the calculated vertical valence excitation energies for the two dimers are even larger than those observed in aqueous solution. These results have convinced us to investigate both the effects of spin−orbit coupling and coupling between the halogen stretch and the intermolecular stretch on the spectra. The results of this study for $H_2O\cdots Cl_2$ are reported in this paper.

II. Method

Given that Cl_2 is the chromophore, and that photodissociation leads to a repulsive $H_2O\cdots Cl_2$ interaction, a 2-D model is the minimum required for a meaningful calculation of the valence excitation spectrum. In addition, a previous study[8] showed that the Cl−Cl and O−Cl coordinates are strongly coupled in both the ground and valence excited states. Here we explore the effects of this coupling on the dimer spectrum within the 2-D model using the wave packet dynamical method and testing the reflection principle and spectator model approximations.

A. Spin−Orbit Addition to PES. A detailed study of the spectroscopic properties of the chlorine molecule must include spin−orbit effects. Among other things the proper description of the dissociation limits for the relevant spectroscopic states (A, B, C) depends crucially on their inclusion. The methodology we have followed has been described in detail in a related study of the $Ne\cdots Cl_2$ system[9] where the spin−orbit effects play a significant role. Here we summarize the main ingredients. We use the relativistic effective core potential (RECP) of chlorine developed by the Stuttgart group[10,11] which provides an efficient way for including spin−orbit effects. The original valence basis set has been extended with polarization and diffuse functions to yield the final set 3s3p3d2f1g. For the water molecule we use the AVTZ (augmented correlation consistent triple-zeta) basis set. The relevant spin−orbit states are obtained by diagonalizing the total Hamiltonian which consists of the usual electronic term plus the spin−orbit interaction term. The basis set for diagonalization is obtained by first optimizing the orbitals in a complete active space (CAS) defined by the valence electrons and orbitals of chlorine, together with a state-averaging of nine electronic states close in energy to the states involved in the spectroscopy. We then perform multireference configuration interaction (MRCI) calculations to include dynamic electron correlation including the valence electrons of the water molecule. The total number of spin−orbit states obtained is 36. All calculations were performed with the MOLPRO2006.1 package.[12]

B. Principle of the Absorption Spectrum Calculation. In this work we determine the $H_2O\cdots Cl_2$ absorption spectrum using a two-dimension model. The coordinates, as described in our previous publication,[8] are the intramolecular Cl−Cl coordinate r and the intermolecular coordinate R (from the center of mass of the water molecule to the center of mass of Cl_2). The other geometrical parameters are fixed at their equilibrium values, with O−Cl−Cl collinear and the hydrogen atoms symmetrically bent off the O−Cl−Cl axis. At $T = 0$ K the Hamiltonian is then

$$H_\beta = -\frac{\hbar^2}{2\mu}\frac{\partial^2}{\partial r^2} - \frac{\hbar^2}{2m}\frac{\partial^2}{\partial R^2} + V_\beta(r,R) \qquad (1)$$

where $\mu = m_{Cl}/2$ and $m = m_{Cl}\, m_{H_2O}/(m_{Cl} + m_{H_2O})$ are the reduced masses associated with r and R, respectively, and $V_\beta(r,R)$ is the two-dimensional potential energy surface in state β with β denoting the X, B, or C electronic state. $V_\beta(r,R)$ is obtained by two-dimension interpolation[13] of the ab initio points of ref 8.

The bound states $\Phi_{xn}(r,R)$ in the X electronic surface are determined by diagonalizing the Hamiltonian matrix in a direct product DVR (discrete variable representation[14−16]) basis set. Each DVR basis set was obtained by diagonalizing the corresponding position operator in an adapted harmonic oscillator basis set (corresponding to the harmonic approximation of the potential minimum). For the sake of comparison with experiment, the vibrationally averaged values of the Cl−Cl distance r_0 and H_2O-Cl_2 center of mass distance R_0 are deduced from the average values of $1/r^2$ and $1/R^2$ over the ground level wave function, respectively. The vibrational frequencies and anharmonicities are obtained from solving the following equation

$$E_{v_r,v_R} = -D_e + \hbar\omega_r(v_r + 1/2) + \hbar\omega_R(v_R + 1/2) - \hbar\omega_r\chi_r(v_r + 1/2)^2 - \hbar\omega_R\chi_R(v_R + 1/2)^2 - \hbar(\omega\chi)_{rR}(v_r + 1/2)(v_R + 1/2) \qquad (2)$$

for the five energy levels E_{00} (≡E_0), E_{10}, E_{01}, E_{11}, E_{02}, adding the minimum energy value of the interpolated surface $D_e = -920.64398$ cm^{-1} ($r_e = 2.0266$ Å, $R_e = 3.9018$ Å) since no $v_r = 2$ level was found.

Since both coordinates are dissociative in the excited state and dissociation is fast, we chose the time-dependent formulation to obtain the absorption spectrum. In this formulation, the absorption spectrum is given by the Fourier transform of the autocorrelation function of a wave packet propagating on the excited state surface. This wave packet is initially determined as the bound state wave function (determined in the previous step) multiplied by the transition dipole moment

$$\Psi_\beta(r,R,t=0) = \mu_{\beta X}(r,R)\Phi_{X_0}(r,R) \qquad (3)$$

We used the split-operator technique with a time step of 1.0 au (2.4×10^{-2} fs) and propagation times of 16000 au (384 fs). The r grid consisted in 256 points from 1.8 to 2.6 Å, the one in R had 256 points running from 3.6 to 16 Å.

One-dimensional absorption spectra were also determined for comparison with gas phase results or for analysis. These were determined as follows. The one-dimensional Hamiltonian reduces to

$$h_\beta = -\frac{\hbar^2}{2\mu}\frac{\partial^2}{\partial r^2} + v_\beta(r) \qquad (4)$$

with

$$v_\beta(r) = V_\beta(r, R_0)$$

where R_0 is a fixed value of the intermolecular coordinate. The X-state bound wave functions $\varphi_v(r)$ were obtained by finite difference[17] followed by Numerov−Cooley[18] integration. The absorption spectra were determined using the time-dependent formulation as described above, or the energy-resolved formulation (coupled channel integration using the De Vogelaere's algorithm[19,20]) for a check.

Cl_2 gas phase absorption spectra were obtained for $R_0 =$ 16 Å, the largest intermolecular distance for which potential energy surfaces were determined. They were compared to spectra obtained from empirical curves fitted to the experimental spectra as a test of the ab initio surfaces.

C. The Spectator Model. The basic assumption of this model is that the water molecule does not have time to move much during the Cl−Cl dissociation. In this case, the sole effect of dimer formation is to modify the potential energy curves of Cl_2. Hence the spectrum can be calculated in one dimension, with the intermolecular distance R fixed at $R_0 = 3.92$ Å (the maximum of the 2-D $H_2O\cdots Cl_2$ wave function) in eq 4. If the predictions of this model are in good agreement with the accurate two-dimension wave packet result, it will prove extremely useful to predict the spectra of Cl_2 in different water environments (clusters, clathrate cages, ice, aqueous solution): the calculation will then reduce to the isolated molecule spectrum but with potential energy curves modified by the environment.

D. The Reflection Principle Method. In analyzing the resulting spectra, we will make reference to the reflection principle. This is an approximation to the absorption cross section that gives very useful physical insight in the case of a dissociative excited state potential. In one dimension the continuum wave function of the excited state β at energy E is simply replaced by a delta function at the classical turning point

$$\chi^\beta_{E,r_0}(r) \simeq \frac{\delta(r - r_0)}{|(\partial V_\beta/\partial r)(r_0)|^{1/2}} \quad (5)$$

with

$$E = V_\beta(r_0)$$

The usual reflection principle formulation for the absorption spectrum is the following

$$\sigma_{\beta\leftarrow X}(E_{ph}) \propto |\langle\chi^\beta_{E,r_0}|\mu_{\beta X}|\chi_{x0}\rangle|^2 \quad (6)$$

where $E_{ph} = E - E_0$ is the photon energy, equal to the energy of the continuum wave function E minus the X bound state energy E_0. It can then be expressed as

$$\sigma_{\beta\leftarrow X}(E_{ph}) \propto \int_0^\infty d\epsilon\, \delta(E - \epsilon)|\langle\chi^\beta_{\epsilon,r_0}|\mu_{\beta X}|\chi_{x0}\rangle|^2 \quad (7)$$

$$= \int_0^\infty dr_0\, \delta(E - V_\beta(r_0))\, |\mu_{\beta X}(r_0)\chi_{x0}(r_0)|^2 \quad (8)$$

where the normalization factor $|(\partial V_\beta\}/\partial r)(r_0)|^{1/2}$ of the delta function disappears because of the change of variable in the integral. Under this form the spectrum is easily determined. A grid is set in r for the ground state wave function and another one in E_{ph} for the spectrum. For each grid point r_i the excited state potential $V_\beta(r_i)$ is calculated and the corresponding $|\mu_{\beta X}(r_i)\chi_{X0}(r_i)|^2$ weight is added to the histogram spectrum at energy $(E_{ph})_j$ closest to $V_\beta(r_i) - E_0$.

The generalization to two dimensions was performed as follows. The two-dimension continuum wave functions were approximated as

$$\Phi^\beta_{\varepsilon,r_0,R_0}(r,R) \simeq \left|\left(\frac{\partial V_\beta}{\partial r}\right)_{r_0,R_0}\left(\frac{\partial V_\beta}{\partial R}\right)_{r_0,R_0}\right|^{-1/2}\delta(r - r_0)\delta(R - R_0) \quad (9)$$

with

$$\varepsilon = V_\beta(r_0, R_0)$$

The absorption spectrum can then be expressed as

$$\sigma_{\beta\leftarrow X}(E_{ph}) \propto \int_0^\infty\int_0^\infty dr_0\, dR_0\, \delta(E - V_\beta(r_0, R_0))\times |\mu_{\beta X}(r_0, R_0)\Phi_{x0}(r_0, R_0)|^2 \quad (10)$$

A grid in (r,R) is set for the ground state wave function and another one in E for the spectrum. For each grid point (r_i,R_j) the excited-state potential $V_\beta(r_i,R_j)$ is calculated and the corresponding $|\mu_{X\beta}(r_i,R_j)\Phi_{X_0}(r_i,R_j)|^2$ weight is added to the histogram spectrum at energy $(E_{ph})_k$ closest to $V_\beta(r_i,R_j) - E_{00}$.

In the limit where the two coordinates are independent also in the ground electronic state and in the transition dipole moment, the spectrum is a simple convolution of the 1D spectra

$$\begin{aligned}\sigma_{\beta\leftarrow X}(E_{ph}) &\propto \int_0^E dE'|\langle\Phi^\beta_{E,E'}(r,R)|\mu_{\beta X}(r,R)|\Phi_{X,0}(r,R)\rangle|^2\\ &= \int_0^E dE'|\langle\chi^\beta_{E',r_0}(r)|\mu^r_{\beta X}(r)|\chi_{X_0}(r)\rangle|^2|\langle\phi^\beta_{E-E',R_0}(R)|\mu^R_{\beta X}(R)|\phi_{X,0}(R)\rangle|^2\\ &= \int_0^E dE'\, \sigma^r_{\beta\leftarrow X}(E' - E_{00})\, \sigma^R_{\beta\leftarrow X}(E - E')\end{aligned} \quad (11)$$

$\sigma^r_{\beta\leftarrow X}$ and $\sigma^R_{\beta\leftarrow X}$ are the $\beta \leftarrow X$ absorption cross sections for the two independent excited state potentials $v_\beta(r)$ and $w_\beta(R)$, respectively, with $v_\beta(r) + w_\beta(R) = V_\beta(r,R)$. Each 1D spectrum being approximated by the reflection principle, the photon absorption cross section is then

$$\sigma_{\beta\leftarrow X}(E_{ph}) \propto \int_0^E dE'\, |\mu^r_{\beta X}[r_0(E')]x^\beta_{X,0}[r_0(E')]\mu^R_{\beta X}[R_0(E - E')]\times \phi^\beta_{X,0}[R_0(E - E')]|^2 \quad (12)$$

where $r_0(E')$ is the classical turning point of the potential $v_\beta(r)$ at energy E' and $R_0(E - E')$ the classical turning point of $w_\beta(R)$ at energy $E - E'$.

III. Results

As stated above, the goal of this study is to calculate the spectrum of $H_2O\cdots Cl_2$ and investigate the effects of spin−orbit coupling, including the Cl−Cl stretch and the $H_2O\cdots Cl_2$ stretch in the calculation. The results for the spin−orbit calculations are presented first, then the ground state calculation is presented and the structure and vibrational frequencies are compared to the previous harmonic results and to available experimental results: the IR spectrum of $H_2O\cdots Cl_2$ recorded in an argon matrix and the spectrum of Cl_2 in an aqueous solution. Finally, the valence excitation spectrum is calculated using the wave packet technique and compared to both the reflection principle approximation and the spectrator model.

A. Effect of Spin−Orbit Interaction. The atomic spin−orbit splitting of Cl is 882.35 cm^{-1} (ref 21). Although this value is not large, the correct description of the B and C states should include these effects in order to properly describe the diatomic dissociation limits and in general for their accurate calculation. For these reasons we thought it important to analyze spin−orbit effects in this system. In Figure 1 we show the geometrical dependence of the spin−orbit correction to the purely electronic states defined as $\Delta E^{SOC}(r,R) = V_\beta^{SOC}(r,R) - V_\beta(r,R)$ where V^{SOC} represents the potential including spin−orbit coupling. In the

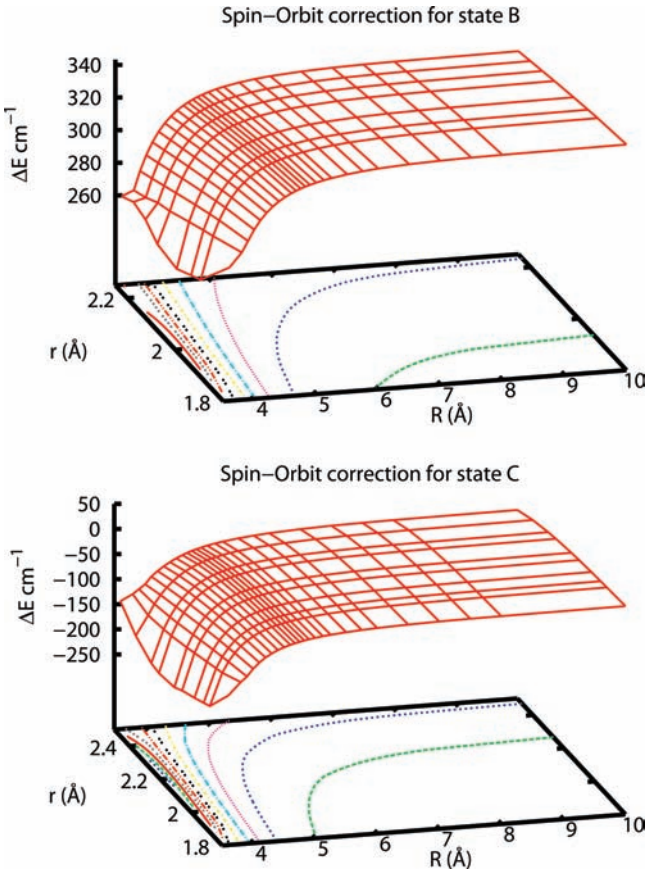

Figure 1. Spin−orbit correction for state B (top) and C (bottom): $\Delta E^{SOC}(r,R) = V_{\beta}^{SOC}(r,R) - V_{\beta}(r,R)$ where V^{SOC} represents the potential including spin−orbit coupling and $V_{\beta}(r,R)$ without. The contour lines are spaced by 10 cm^{-1} for the B state and 20 cm^{-1} for the C state.

case of the B state (top part of Figure 1) the correction is positive as expected since the corresponding $^3\Pi_u$ electronic state splits into the lower A and the higher B spin−orbit states upon inclusion of the spin−orbit coupling. There is a marked dependence on the intermolecular distance leading to a monotonic decrease of ΔE^{SOC} as the interaction potential increases. The dependence with the chlorine internuclear distance is weaker with a monotonic decrease in ΔE^{SOC} as r increases. For the C state (bottom part of Figure 1) the absolute values of ΔE^{SOC} are smaller and the geometrical dependence is qualitatively similar to that of the B state. Interestingly the values of ΔE^{SOC} change sign when moving from the $Cl_2 + H_2O$ asymptotic value toward the interaction region (the most external contour in the bottom plot of Figure 1 is zero).

One of the main consequences of spin−orbit in the spectra should be a decrease in the energy separation between the B and C absorption bands. Because the separation between the B and C states is already large without including the spin−orbit coupling; the intensity to the B state is quite low; and the spin−orbit shift for the C state in the Franck−Condon region is less than 100 cm^{-1}, the spin−orbit effects on the calculated spectrum are not substantial in this case. However, since spin−orbit correction is not constant throughout the surface, other more subtle effects that depend on the intermolecular interactions could be observed in high resolution spectra with detailed information about the van der Waals bound levels for the B state.

B. $H_2O\cdots Cl_2$ Bound States. Results for the $H_2O\cdots Cl_2$ vibrational levels of the ground electronic state obtained using the surface formed from the ab initio points of ref 8 are presented

TABLE 1: Bound State Results for the X Electronic State of $^{35}Cl_2$ and of the $H_2O\cdots{}^{35}Cl_2$ Complex, Compared to Experimental Spectroscopic Data[h]

	calculated values		experimental values	
	Cl_2	$H_2O\cdots Cl_2$	Cl_2	$H_2O\cdots Cl_2$
E_0 (cm^{-1})	268.717	−605.245		
r_0 (Å)	2.0225	2.0296	1.9915[a]	(1.9915)[b]
R_0 (Å)		3.9251		4.2907[c]
$\hbar\omega_r$ (cm^{-1})	541.560	531.339	559,72[d]	543.3[e], 538[f]
$\hbar\omega_r\chi_r$ (cm^{-1})	2.402	2.306	2.717[d]	
$\hbar\omega_R$ (cm^{-1})		101.952		97.4(6)[g]
$\hbar\omega_R\chi_R$ (cm^{-1})		3.218		
$\hbar(\chi\omega)_{rR}$ (cm^{-1})		−0.538		

[a] Reference 29. [b] Fixed to the monomer value in order to deduce R_0, ref 30. [c] Obtained from $\langle R_{OCl}\rangle = 2.8479$ Å in ref 30. [d] Reference 31. [e] $H_2O\cdots Cl_2$ in argon matrices, ref 32. [f] Cl_2 in aqueous solution, ref 33. [g] From $k_\sigma = 8.0(1)$ N m^{-1} in ref 30. [h] E_0 is the energy of the zero-point level (the zero for energies is the minimum of the ab initio Cl_2 potential energy curve without water; the minimum of the interpolated Cl_2 potential energy curve is −1.573 cm^{-1} at (r = 2.0194 Å, R = 15 Å)). For the determination of r_0 and R_0 and of the vibrational frequencies and anharmonicities, see text and eq 2.

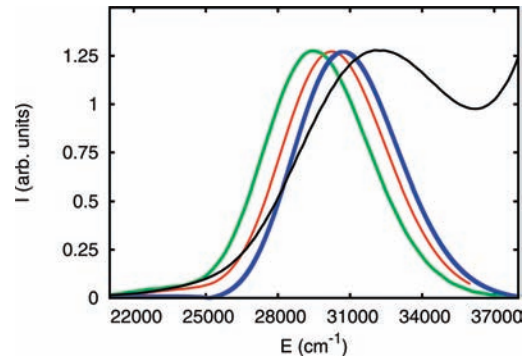

Figure 2. Cl_2 (green line) and $H_2O\cdots Cl_2$ (blue line) absorption spectrum determined by wave packet propagation using ab initio potentials. Comparison with spectrum at 0 K using empirical ("RKR") potentials (red line) and with spectrum in liquid water at 300 K[3] (black line).

in Table 1. Since the present calculation explicitly includes anharmonicity, the vibrational frequencies are lower than those reported in ref 8. The calculated value for the Cl_2 bond length in the free molecule is within 1.5% of that of the gas phase experimental value. The bond lengthens only slightly, 0.007 Å, upon formation of the dimer. The R intermolecular bond length (center of mass distance) is calculated to be 3.925 Å, slightly shorter than the vibrationally averaged experimental value 4.291 Å. The calculated Cl−Cl stretching frequency falls from 541.6 cm^{-1} in the free molecule to 531.3 cm^{-1} in the $H_2O\cdots Cl_2$ dimer. These values compare to the experimental gas phase value for Cl_2, 559.7 cm^{-1}, the experimental value for Cl_2 in aqueous solution, 538 cm^{-1}, and the experimental value for $H_2O\cdots Cl_2$ in an argon matrix, 543.3 cm^{-1}. It is also interesting to note that the calculated anharmonicity for this mode drops slightly in going from the gas phase to the $H_2O\cdots Cl_2$ dimer. The calculated value for the intermolecular stretch, 102.0 cm^{-1}, is in good agreement with the value estimated from centrifugal distortion in the molecular beam study, 97 cm^{-1}.

C. $H_2O\cdots Cl_2$ Spectra. The calculated spectra for Cl_2 and $H_2O\cdots Cl_2$ using the 1- and 2-D wave packet methods and the ab initio potentials are shown in Figure 2 along with the spectrum calculated from the Cl_2 RKR potentials[22,23] and the experimental spectrum for Cl_2 in aqueous solution. For each of the spectra except the 2-D wavepacket calculation the red tail

TABLE 2: Calculated Absorption Maxima, Shifts, And Widths (cm^{-1}) for the $H_2O\cdots Cl_2$ Complex C ← X Absorption Spectrum, Compared to Experimental Results for Cl_2 in Different Water Environments

environment	absorption max. (cm^{-1})	shift (cm^{-1})	width (cm^{-1})
empirical gas phase	30302	0	5076
ab initio gas phase 1D wave packet	29467	0	5090
ab initio 1D vertical	29725	0	
ab initio gas phase 1D reflection principle	29102	0	5110
ab initio 2D wave packet	30719	1252	5020
ab initio 2D vertical	30904	1179	
ab initio 2D reflection principle	30010	908	5080
ab initio 2D spectrator model	30471	1087	5080
$5^{12}6^2$ cage[a]	30300	≃0	≃5076
aqueous solution	30850	550	

[a] Reference 3.

of the spectrum is due to the relatively weak B ← X transition and the main peak is due to the more intense C ← X spectrum. Only the C ← X spectrum was calculated in the case of the 2-D wavepacket. Since the C state of Cl_2 is purely dissociative, the C ← X absorption spectrum is broad and structureless. The shifts of the peak positions of the $H_2O\cdots Cl_2$ spectra, relative to the value for Cl_2 at the same level of approximation, are given in Table 2.

The peak of the ab initio Cl_2 spectrum is at 29470 cm^{-1}, within 800 cm^{-1} of the experimental value. In this sense the C state ab initio surface is quite satisfactory. The blue shift of the ab initio dimer spectrum, relative to that of the free molecule, each calculated with the wave packet method, is 1250 cm^{-1}. Seventy percent of the blue shift can be attributed to the $H_2O\cdots Cl_2$ bond in the ground electronic state: $E_0(Cl_2) - E_0(H_2O\cdots Cl_2) = 875$ cm^{-1}. Most of the rest is due to the repulsive $H_2O\cdots Cl_2$ interaction in the C state.

The shift estimated from the vertical excitation energy deduced directly from the interpolated potential energy surfaces, 1180 cm^{-1}, is close to the wave packet result, but this good agreement is actually due to a compensation of errors. Taking into account the bound state zero point energy would give a lower energy, and the fact that the maximum of the excited state wave function is at slightly larger values than the classical turning point gives a correction in the opposite direction. Note that the difference with the vertical excitation energy of 1554 cm^{-1} in our previous work[8] originates from the strong slope of the excited state potential with the halogen coordinate: the 2D-interpolated surface has its minimum at $r_e = 2.0266$ Å whereas the ab initio vertical excitation energy was calculated at 2.02 Å.

Although it is possible to do an accurate 2-D wave packet simulation of the spectrum for the $H_2O\cdots Cl_2$ dimer, in subsequent studies we will examine larger clusters and also try to simulate the spectra in solution. Thus, we examined more appoximate calculations of the spectra for this model system. Spectra calculated using the reflection principle and the spectator model are shown in Figure 3. Both the reflection principle and the spectator model yield spectra that are less shifted to the blue relative to the more accurate wave packet calculation. The reflection principle calculation underestimates the blue shift upon dimer formation by 340 cm^{-1} and the spectator model by 160 cm^{-1}. Each of the approximate methods predicts a spectrum width that is slightly larger than the wave packet result.

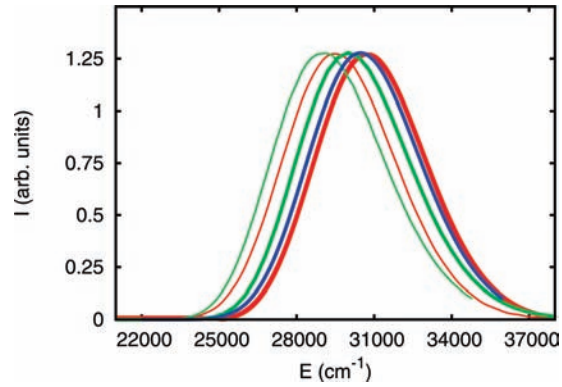

Figure 3. Comparison of Cl_2 (thin lines) and $H_2O\cdots Cl_2$ (bold lines) C ← X absorption spectra obtained using the reflection principle (green lines) and the spectator model (blue line) with the ones determined by wave packet propagation (red lines). All spectra are using the C ab initio potential.

IV. Discussion

As discussed previously,[8] the strong blue shift in the $H_2O\cdots Cl_2$ dimer spectrum is due to strong intermolecular bonding in the ground electronic state and Franck−Condon excitation to a repulsive region of the excited electronic state. The results above show that slightly more than two-thirds of the shift is due to the ground state and the rest to the excited state. The unusual intermolecular forces between electron-donating molecules and the dihalogens has long been noted and it has recently been suggested that this bonding deserves its own name: halogen bonding.[24,25] Typical halogen bonds are somewhat weaker than typical hydrogen bonds, but much stronger than typical van der Waals and electrostatic bonds. As for hydrogen bonding, considerable discussion has been devoted to the proper interpretation of the strong halogen bonds. Pictorially, they result from a strong HOMO−LUMO overlap between the oxygen lone pair and the halogen σ^* orbital. However, this configuration is also ideal for optimizing the electrostatic interactions. Also, the "dimple" in the repulsive wall on the ends of the halogen molecules leads to large dispersion−attraction in this configuration. Upon valence electronic excitation, each of these advantages of the ground state structure disappears, along with an increase in the halogen bond length, leading to a net repulsion in the Franck−Condon region and a strong blue shift.

A. Spectrum Shift. It is particularly interesting that the calculated blue shift for the $H_2O\cdots Cl_2$ dimer is significantly greater than that observed in aqueous solution as well as in the clathrate hydrate. In aqueous solution, the blue shift is 550 cm^{-1}, less than half of the $H_2O\cdots Cl_2$ dimer blue shift. Although the detailed interpretation of this result is yet to be developed, it seems likely that in the condensed phase systems the optimal geometry for strongly attractive halogen bonding forces does not significantly contribute to the ensemble average. Even though the $H_2O\cdots Cl_2$ bond is quite strong, it is still 300 cm^{-1}

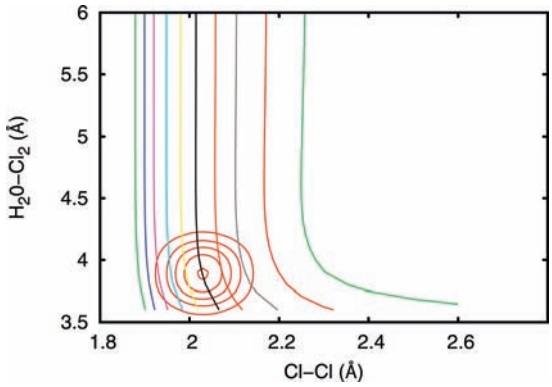

Figure 4. $H_2O\cdots Cl_2$ initial wave packet superimposed on the C state equipotentials, revealing the difference in slope along the r (Cl−Cl) and R (H_2O−Cl_2 center of mass distance) coordinates in the Franck−Condon region. Potential values are from 22000 to 40000 cm^{-1} by 2000 cm^{-1}; wave function values are from 1 to 5 in $Å^{-1/2}$.

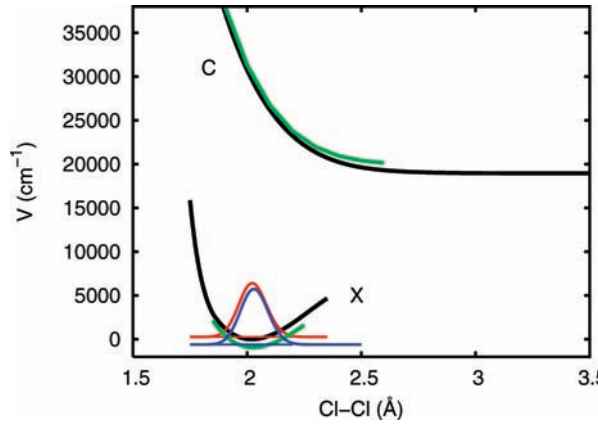

Figure 5. Cl_2 X and C curves without (black curves) or with (green curves) water at equilibrium distance. Also shown is the (X, $v = 0$) bound state wave function of Cl_2 without (red curve) or with (blue curve) water at equilibrium distance. The most important difference in the Franck−Condon region is the bound state energy. Note also the slight lengthening of the Cl−Cl bond upon dimer formation and the relative flattening of the C state repulsive wall in the Franck−Condon region.

less strong than the H_2O−H_2O hydrogen bond.[26] Thus we expect that the actual halogen bond formation in aqueous solution is quite rare.

In the hydrate−clathrate cage, all of the water molecule lone electron pairs are involved in hydrogen bonding and, indeed, no blue shift at all is observed. Presumably there is still some weaker $H_2O\cdots Cl_2$ ground-state attraction in the cages since the halogen molecule provides the net stability that allows the clathrate hydrates to form. Schofield and Jordan[27] calculated the lowest singlet electronic excitation for free Cl_2 and in a single 5^{12} cage at the CC2/AVDZ level and obtained a red shift of 550 cm^{-1}. The question arises whether long-range dielectric effects like the bulk dielectric constant of the solvent may contribute a red shift to the spectrum. Preliminary reaction field calculations that take into account the bulk dielectric constant for a chlorine molecule in a water cavity indicate a red shift of 550 cm^{-1}. As accurate model potentials become available, it will be interesting to determine the effects of nearest neighbors, other cage molecules, and the molecules and adjacent cages on the halogen spectra.

B. Spectral Widths. Although so far we have been concentrating on the peak positions of the spectra, the widths of the spectra also yield useful information concerning the effective potentials. In this regard it is especially interesting that the 2-D spectrum of the $H_2O\cdots Cl_2$ dimer calculated with the ab initio potentials is actually narrower than that calculated for free Cl_2 at the same level of approximation. This result persists in the reflection principle and spectator model approximations. In the limit of two independent coordinates the reflection principle would predict that the width of the dimer spectrum would be a simple convolution of the widths due to the Cl−Cl coordinate, r, and the width due to the $H_2O\cdots Cl_2$ intermolecular coordinate, R. However, as shown in Figure 4, Franck−Condon excitation of the ground state wave function onto the C state surface creates a wave packet that is strongly repulsive on r but only weakly repulsive on R. Thus the wave packet will quickly move on r without having much chance to spread on R. This insight may help interpret spectral broadening in condensed phase systems.

The different levels of repulsion in r and R would predict that the $H_2O\cdots Cl_2$ dimer spectrum would be only slightly broader than the free Cl_2 spectrum. The fact that it is actually slightly narrower can be explained by the potential curves and wave function shown in Figure 5. Two effects serve to slightly narrow the spectrum. First, the ground-state wave function in the dimer is centered at slightly larger r values than in the free Cl_2 molecule. Second, although the C state repulsion is longer range in the dimer than in the free Cl_2 molecule, it is somewhat flatter. It would be very interesting if this change in the C state potential could be confirmed by experimental spectra on the dimer. It also remains to be seen how the other degrees of freedom affect this result.

In a recent experimental work on Br_2 in ice,[28] a very large broadening was found. It was attributed to homogeneous broadening, which implied a very repulsive $H_2O\cdots Br_2$ interaction in the excited states. To the extent that the spectrum in ice is due to halogen bonding analogous to that studied here, our results suggest that the broadening contains a substantial inhomogeneous component. Figure 5 presents the X and C Cl_2 curves without water and with a water molecule at equilibrium distance. The most important change is the lowering of the bound state energy. The excited-state potential is not very displaced, and if anything its slope is slightly smaller which gives a smaller width as discussed above. On the other hand, inhomogeneous broadening resulting from the superposition of $H_2O\cdots Br_2$ absorptions in a variety of configurations could contribute substantially to the broadening. Assuming that the interval between two successive water−bromine collisions is on average of the same order or larger than the average lifetime of a $H_2O\cdots Br_2$ complex, the incoming photon could interrogate Br_2 with a water molecule at any distance. Since the main effect of the water molecule is to displace the ground state energy, the result would be a shift varying between 0 and about 1500 cm^{-1}, which would appear as a broadening of the order of 1500 cm^{-1}. Clearly, the interpretation of these results will require more detailed studies.

C. Spectator Model. Figure 3 shows the C ← X absorption spectrum of $H_2O\cdots Cl_2$ using the spectator model presented in section II.C. On the basis of the result that the water molecule does not have time to move much during the Cl···Cl dissociation (section IV.B), it is expected to give accurate results. Indeed, the resulting spectrum is very close to the spectrum obtained using two-dimension wave packet propagation. As can be also seen in Table 2, there is only a difference of 165 cm^{-1} in the shift and 60 cm^{-1} in the width, indicating that it is a good approximation. That the spectator model is quite accurate with regard to both the position of the spectrum and its width should

prove to be very useful for the interpretation of the spectra in larger clusters and condensed phase systems.

D. 2-D Reflection Principle Results. Figure 3 also shows the C ← X absorption spectrum of Cl_2 and $H_2O\cdots Cl_2$ using the 1-D and 2-D reflection principle, respectively. The corresponding shift and widths are collected in Table 2. The agreement with the wave packet result is good, although less so than in the spectator model for the shift. This is due to the fact that the continuum wave function is not entirely localized at the classical turning points. But the widths are also in very good agreement with the ones determined using wave packet propagation. This validates the physical interpretation of the large shift and slight narrowing of the dimer spectrum presented above.

E. Further Studies. In this paper we have calculated the valence excitation spectra for the $H_2O\cdots Cl_2$ dimer using near state-of-the-art 2-D potentials and several levels of dynamics approximation. We expect the current calculations to be quite accurate with respect to the shifts and widths of the spectra for this 2-D model. However, the effect of the other intermolecular coordinates remains to be explored. Also, there are no experimental spectra available for direct comparison to our results. It will be especially satisfying if experiment could confirm that the width of the dimer spectrum is slightly less than that of the free Cl_2. For $H_2O\cdots Cl_2$ spin−orbit effects are found to be minor, except at very small intermolecular distances and, of course, to offset the B and C state dissociation limits. Spin−orbit effects may still be important for $H_2O\cdots Br_2$ and $H_2O\cdots I_2$. For instance, for these two dimers the B → X transition becomes much more intense than for $H_2O\cdots Cl_2$. For subsequent studies of larger clusters and condensed phase systems it is very promising that the spectator model yielded a quite satisfactory approximation to the wave packet calculation. In the experimental spectrum of aqueous Cl_2 strong charge transfer bands interfere with the analysis of the valence band, as shown in Figure 2. This difficulty should be less important for the Br_2 and I_2 systems for which the valence bands occur at much lower energies.

V. Conclusion

Valence electronic excitation spectra have been predicted for a 2-D model of the $H_2O\cdots Cl_2$ dimer. Although the calculated spectrum for Cl_2 is 1000 cm^{-1} red-shifted from the experimental spectrum, we expect that the calculated effects of dimer formation are accurate enough to quantitatively compare to an eventual experiment. We found that the blue shift for the dimer spectrum is smaller than that previously estimated based on vertical excitation energies but still significantly larger than for Cl_2 in aqueous solution and in clathrate hydrate cages. This effect should persist in a more complete calculation including other degrees of freedom of the dimer: although the dimer blue shift may be smaller than that calculated here, it will still be larger than that in aqueous solution. Future studies may be able to determine what fraction of the difference between the dimer and condensed phase spectra is due to nearest neighbor geometry and what fraction is due to longer range and many-body effects. A particularly interesting result of this study is that the width of the calculated dimer spectrum is less than that of the free molecule. This was attributed to subtle changes in the r and R potentials upon dimerization. Also, since the repulsion along the R coordinate is much less steep than that along the r coordinate in the region of Franck−Condon excitation, little homogeneous broadening due to the nearest neighbor interactions is expected even in condensed phase experiments. It was found that both the reflection principle and, especially, the spectator model yield excellent approximations to the more accurate wave packet calculation. This is very encouraging for the eventual simulation of condensed phase spectra.

Acknowledgment. Benny Gerber has worked on numerous subjects during his career and his work has always been inspiring. This work relates to only a few of them: water clusters, electronic spectra of dihalogen molecules in condensed phase, and bound state calculations for wide amplitude vibrations. The authors thank A. Apkarian for stimulating discussions, especially concerning the implications of this work for condensed phase spectra. This project was supported by NSF-CONACYT J110.385 and the NSF Grant CHE-0404743. NH and KCCJ would like to thank CNRS for a collaboration grant (PICS 4648). Computer time has been provided by the laboratories of the authors, the CALMIP computer center of Toulouse, the CINES national computer center of Montpellier, and the IDRIS national computer center of Paris.

References and Notes

(1) Bayliss, N. S. *J. Chem. Phys.* **1950**, *18*, 292.
(2) Buckles, R. E.; Mills, J. F. *J. Am. Chem. Soc.* **1953**, *75*, 552.
(3) Janda, K. C. Kerenskaya, G. Goldschleger, I. U. Apkarian, V. A., and Fleischer, E. B. In *Proceedings of the 6th International Conference on Gas Hydrates (ICGH 2008), Vancouver, British Columbia, Canada, July 6−10, 2008* (The University of British Columbia, 2008. URL https://circle.ubc.ca/bitstream/2429/1476/1/5393.pdf.
(4) Kerenskaya, G.; Goldschleger, I. U.; Apkarian, V. A.; Janda, K. C. *J. Phys. Chem. A* **2006**, *110*, 13792.
(5) Kerenskaya, G.; Goldschleger, I. U.; Apkarian, V. A.; Fleischer, E.; Janda, K. C. *J. Phys. Chem. A* **2007**, *111*, 10969.
(6) Geilhaupt, M.; Dorfmuller, T. *Chem. Phys.* **1983**, *76*, 443.
(7) Renger, T.; Grundkötter, B.; Madjet, M. E.; Müh, F. *Proc. Natl. Acad. Sci. U.S.A.* **2008**, *105*, 13235.
(8) Hernández, R.; Uc Rosas, V. H.; Bernal Uruchurtu, M. I.; Halberstadt, N.; Janda, K. C. *J. Phys. Chem. A* **2008**, *112*, 89.
(9) Hernández, R.; Janda, K. C. *J. Chem. Phys.* **2005**, *123*, 161102.
(10) Dolg, M. Ph.D. thesis, University of Stuttgart, 1989.
(11) Bergner, A.; Dolg, M.; Kuechle, W.; Stoll, H.; Preuss, H. *Mol. Phys.* **1993**, *80*, 1431.
(12) Amos, R. D. ; et al. Molpro, a package of ab initio programs designed by H.-J. Werner and P. J. Knowles, version 2006.1.
(13) Press, W. H. Flannery, B. P. Teukolsky, S. A., and Vetterling, W. T. *Numerical Recipes in Fortran: The art of scientific computing*; Cambridge University Press: Cambridge, 1986−1992.
(14) Lill, J. V.; Parker, G. A.; Light, J. C. *Chem. Phys. Lett.* **1982**, *89*, 483.
(15) Heather, R. W.; Light, J. C. *J. Chem. Phys.* **1983**, *79*, 147.
(16) Bačić, Z.; Light, J. C. *J. Chem. Phys.* **1986**, *85*, 4594.
(17) Truhlar, D. G. *J. Comput. Phys.* **1972**, *10*, 123.
(18) Cooley, J. W. *Math. Comp.* **1961**, *15*, 363.
(19) Lester, W. *J. Comput. Phys.* **1968**, *3*, 322.
(20) Lester, W. *Methods Comput. Phys.* **1971**, *10*, 211.
(21) NIST Handbook of Basic Atomic Spectra, http://physics.nist.gov/PhysRefData/Handbook/Tables/chlorinetable5.htm.
(22) Coxon, J. A. *J. Mol. Spectrosc.* **1980**, *82*, 264.
(23) Burkholder, J. B.; Bair, E. J. *J. Phys. Chem.* **1983**, *87*, 1859.
(24) Legon, A. C. *Chem.−Eur. J.* **1998**, *4*, 1890.
(25) Legon, A. C. *Angew. Chem.* **1999**, *111*, 2850.
(26) Mas, E. M.; Bukowski, R.; Szalewicz, K.; Groenenboom, G. C.; Wormer, P. E. S.; van der Avoird, A. *J. Chem. Phys.* **2000**, *113*, 6687.
(27) Schofield, D. P.; Jordan, K. D. *J. Phys. Chem. A* **2007**, *111*, 7690.
(28) Goldschleger, I. U.; Senekerimyan, V.; Krage, M. S.; Seferyan, H.; Janda, K. C.; Apkarian, V. A. *J. Chem. Phys.* **2006**, *124*, 204507.
(29) Edwards, H.; Long, D. A.; Mansour, H. R. *J. Chem. Soc., Faraday Trans. 2* **1978**, *74*, 1200.
(30) Davey, J. B.; Legon, A. C.; Thumwood, J. M. A. *J. Chem. Phys.* **2001**, *114*, 6190.
(31) Coxon, J. A.; Shanker, R. *J. Mol. Spectrosc.* **1978**, *69*, 109.
(32) Engdahl, A.; Nelander, B. *J. Chem. Phys.* **1986**, *84*, 1981.
(33) Cherney, D. P.; Duirk, S. E.; Tarr, J. C.; Collette, T. W. *Appl. Spectrosc.* **2006**, *60*, 764.

JP901488X